

Electron-spin phase relaxation of phosphorus donors in nuclear-spin-enriched siliconEisuke Abe,¹ Kohei M. Itoh,^{1,*} Junichi Isoya,² and Satoshi Yamasaki³¹*Department of Applied Physics and Physico-Informatics, Keio University, and CREST-JST, 3-14-1 Hiyoshi, Yokohama 223-8522, Japan*²*Research Center for Knowledge Communities, University of Tsukuba, 1-2 Kasuga, Tsukuba City 305-8550, Japan*³*Diamond Research Center, National Institute of Advanced Industrial Science and Technology, Tsukuba Central 2, 1-1-1 Umezono, Tsukuba City 305-8568, Japan*

(Received 4 February 2004; revised manuscript received 23 March 2004; published 26 July 2004)

We report a pulsed electron paramagnetic resonance study of the phase relaxation of electron spins bound to phosphorus donors in isotopically purified ^{29}Si and natural abundance Si ($^{\text{nat}}\text{Si}$) single crystals measured at 8 K. The two-pulse echo decay curves for both samples show quadratic dependence on time, and the electron phase relaxation time T_M for ^{29}Si is about an order of magnitude shorter than that for $^{\text{nat}}\text{Si}$. The orientation dependence of T_M demonstrates that the phase relaxation is caused by spectral diffusion due to flip-flops of the host nuclear spins. The electron spin echo envelope modulation effects in ^{29}Si are analyzed in the frequency domain.

DOI: 10.1103/PhysRevB.70.033204

PACS number(s): 76.30.-v, 03.67.Lx, 28.60.+s, 76.60.Lz

Group-V impurities in silicon have been studied extensively in semiconductor physics. Experimental techniques such as infrared absorption, photoluminescence, and electron paramagnetic resonance (EPR) have revealed detailed properties of the impurity centers. EPR is particularly convenient for the identification of defect structures since the hyperfine (hf) interaction is a sensitive probe of the spatial distribution of the electron wave function. For instance, Feher and later Hale and Mieher applied an electron nuclear double-resonance (ENDOR) technique to this system, and measured hf interactions between the donor electron spins and their neighboring host nuclear spins.^{1,2} These experimental works, together with theoretical investigations,^{3,4} have deepened our understanding of shallow donor impurities.

Recently, Kane and others gave a new perspective to the donors in Si, a playground for solid-state quantum information processing, since nuclear and electron spins in semiconductors can be regarded as well-isolated two-level systems: qubits.⁵⁻⁷ If the donor electrons are qubits, ^{29}Si nuclei that have spin-1/2 and occupy 4.67% of the lattice sites in natural Si ($^{\text{nat}}\text{Si}$) are decoherence sources as their flip-flops produce fluctuations of the local fields. Indeed, ^{29}Si -depleted, isotopically controlled $^{28}\text{Si}:\text{P}$ exhibited the coherence time two orders of magnitude longer than $^{\text{nat}}\text{Si}:\text{P}$,^{8,9} demonstrating that such nuclear spin-diluted Si would be indispensable for building a practical Kane-type quantum computer. On the other hand, a study of the decoherence caused by the spectral diffusion arising from nuclear flip-flops requires a material of the opposite class, nuclear spin-enriched Si. This novel material is also interesting because of its similarity to III-V materials in that the electrons are localized in a sea of nuclear spins, and more preferable for our purpose owing to the negligibly small spin-orbit interaction in bulk Si, which could otherwise contribute to decoherence.

In this paper, we report the phase relaxation time T_M for P donor electron spins in isotopically purified ^{29}Si and $^{\text{nat}}\text{Si}$ measured at 8 K. The temperature was chosen so that T_M would not be affected by the spin-flip time T_1 . The ground-

state electron can be excited by absorbing a phonon if the phonon energy is comparable to the transition energy from the A_1 ground state to the E or T_2 excited states. When returning to the ground state, the electron is subject to a spin-flip at a certain probability. This T_1 process, known as an Orbach process, also limits T_M over the temperature range from 10 to 20 K.^{9,10} While T_1 is dominated by the Orbach process down to 6 K, and extends exponentially with cooling,^{11,12} T_M starts to deviate from T_1 and becomes insensitive to the temperature below about 10 K.^{9,10} Since our spin echo experiments require each pulse sequence to be repeated at time intervals much longer than T_1 , we found 8 K to be an appropriate temperature, low enough for T_M not to be limited by T_1 but high enough to ensure a reasonable measuring time.

A Cz-grown single crystal of ^{29}Si , enriched to 99.23%, had a rectangular shape with its long axis in the $[\bar{1}\bar{1}0]$ orientation. The sample contained 1.8×10^{15} P/cm³ with the compensation of 1.0×10^{15} B/cm³. Further information on this crystal is provided in Ref. 13. A $^{\text{nat}}\text{Si}$ sample was cleaved from a commercial high-quality wafer containing 0.8×10^{15} P/cm³ with a negligible amount of compensation. The net donor concentrations of both samples were kept low so that the dipolar or exchange interactions between donors would be suppressed.^{14,15} Pulsed experiments were carried out using a Bruker Elexsys E580 spectrometer, and samples were kept in an Oxford ER4118CF cryostat. Temperature was controlled with an Oxford ITC503 temperature controller. The echo-detected EPR spectra, in which the intensity of the Hahn echo was measured as a function of the external magnetic field, consisted of two Gaussian-shaped lines separated by 4.2 mT. The splitting is due to the hf interaction with ^{31}P , and each line is inhomogeneously broadened by the surrounding ^{29}Si nuclei. The linewidths (FWHM) are 0.26 mT for $^{\text{nat}}\text{Si}$ and 1.2 mT for ^{29}Si . In the following experiments, the external magnetic field was set to the center of the line at higher fields ($B_0 = 348$ mT). T_1 was measured using an inversion recovery method (π - t - $\pi/2$ - τ - π - τ -echo),

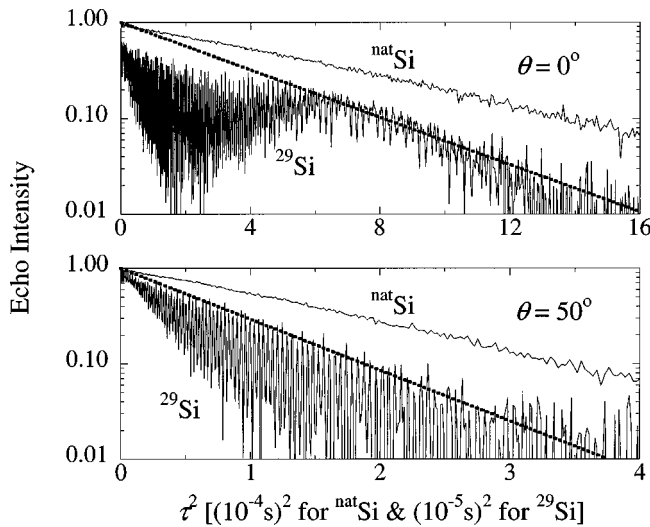


FIG. 1. The two-pulse electron spin echo decay curves as a function of τ^2 at $\theta=0^\circ$ and 50° . Note that the unit of the horizontal axis differs for each sample, and the scale for each θ . The straight dotted lines are the fits to the echo envelope decays of ^{29}Si . The oscillation observed in ^{29}Si is ESEEM. See the text.

and is 16 ms for $^{\text{nat}}\text{Si}$ and 4.4 ms for $^{\text{nat}}\text{Si}$. As the temperature dependence of the Orbach process is given by $1/T_1 = R \exp(-\Delta/kT)$, where R is the rate constant and Δ the valley-orbit splitting energy, the difference in T_1 between samples could arise in part from a slight difference in the actual sample temperatures. The isotope shift of Δ is unlikely to cause the difference in T_1 , since it was not observed in our infrared photoconductivity measurement on the ^{29}Si crystal within the resolution used.¹³ The presence of compensation and dislocation (10^2 cm^{-2}) in the ^{29}Si crystal can alter T_1 , changing R .^{16,17} However, we can conclude that this difference in T_1 has little effect on the difference in T_M presented below, based on the previous assumption that T_1 does not contribute to T_M .

The phase relaxation was investigated using a two-pulse spin echo method ($\pi/2$ - τ - π - τ -echo, where the interpulse delay τ was varied in 800-ns steps for $^{\text{nat}}\text{Si}$ and 40-ns steps for ^{29}Si . The duration of the $\pi/2$ pulse was 16 ns). The samples were rotated around the $[1\bar{1}0]$ axis perpendicular to \mathbf{B}_0 . We define θ as the angle between \mathbf{B}_0 and $[001]$; therefore, $\theta=0^\circ$ when $\mathbf{B}_0 \parallel [001]$, $\theta=55^\circ$ when $\mathbf{B}_0 \parallel [111]$ and $\theta=90^\circ$ when $\mathbf{B}_0 \parallel [110]$. Since the echo-detected EPR spectra were independent of the crystal orientation, and no other EPR signals were found, the alignment of the crystal from an EPR signal was not applied here. We estimate the uncertainty in θ to be less than 5° . Figure 1 shows the echo decay curves at $\theta=0^\circ$ and 50° . Although so-called electron spin echo envelope modulation (ESEEM) obscures the echo envelope decays, they clearly obey a quadratic decay law, expressed as $\exp(-m\tau^2)$. A single-exponential term $\exp(-2b\tau)$ is, if present at all, quite small. Thus, T_M can be defined as the time at which an echo envelope damps to $1/e$ of its initial value, i.e., $T_M = 2m^{-1/2}$. We note that our temperature setting and assumption on the T_1 effect are justified *a posteriori* by the fact that the echo decay curves are not single exponential

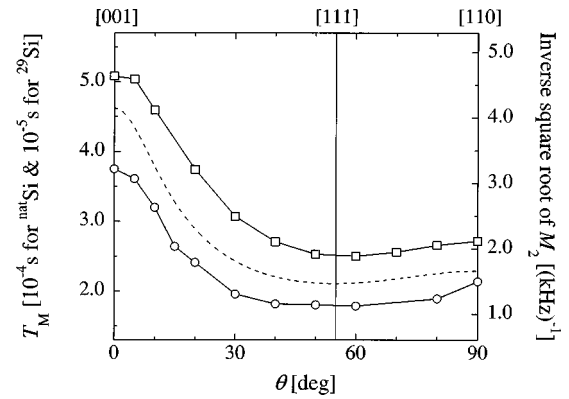


FIG. 2. The orientation dependence of T_M for $^{\text{nat}}\text{Si}$ and ^{29}Si (left axis). The open squares (\square) represent T_M for $^{\text{nat}}\text{Si}$, and the open circles (\circ) for ^{29}Si . Note that the unit of the vertical axis differs for each sample. The inverse square root of M_2 calculated based on the method of moment is also shown by a dashed line (right axis).

and that T_M for each sample is much shorter than the respective T_1 .

The orientation dependence of T_M given in Fig. 2 shows T_M to be longest at $\theta=0^\circ$, and shortest around $\theta=50^\circ-60^\circ$.¹⁸ The dependence manifests the fact that the phase relaxation is caused by ^{29}Si nuclei mutually coupled via the dipolar interactions. This can be verified by calculating the second moment M_2 of the ^{29}Si nuclear spin system. M_2 calculated with Van Vleck's method of moment is the sum of squared dipolar fields produced by the nuclei,¹⁹ and its inverse square root is a convenient measure of the nuclear T_2 . $(M_2)^{-1/2}$ for a 100% ^{29}Si crystal is shown in Fig. 2 by a dashed line. Correlations between the electron T_M and the nuclear M_2 are apparent. As M_2 directly reflects the strength of the nuclear dipolar couplings, its orientation dependence is understood qualitatively as follows: When \mathbf{B}_0 is along $[111]$, one of the four nearest-neighbor bonds of the Si atoms is parallel to \mathbf{B}_0 , and this pair of nuclei gives rise to the strongest coupling; hence, M_2 takes its maximum. With \mathbf{B}_0 along $[001]$, all the dipolar couplings between nearest neighbors are frozen since the angle between \mathbf{B}_0 and the vector connecting the nearest neighbors is a so-called magic angle; hence, M_2 takes its minimum. In fact, such an experimental T_2 has been reported for NMR of ^{13}C diamond, a material similar to ^{29}Si .²⁰ As the line shape studies of NMR spectra for ^{13}C diamond and ^{29}Si have revealed that they share essentially the same line-broadening mechanism, T_2 for ^{29}Si will show the same tendency as that for ^{13}C diamond if measured.^{21,22}

Although the comparison with M_2 works qualitatively, it provides little information on the actual value of T_M . Theoretical estimation of T_M must take the hf interaction between the electron and host nuclei into account, as well as the nuclear dipolar coupling. Generally, to characterize a system where the electron phase relaxation is caused by the spectral diffusion due to flip-flops of the host nuclear spins, the diffusion barrier that prevents the flip-flops within its bounds must be considered.²³ As the Fermi contact hf interaction, which is proportional to the density of the electron wave function $|\Psi(\mathbf{r}_i)|^2$, varies from site to site, a flip-flop of a certain pair of nuclei occurs only when the difference of the

hf interaction between the pair is small enough to satisfy the condition of energy conservation. The condition must be evaluated for each pair, since $|\Psi(\mathbf{r}_i)|^2$ does not decrease monotonically with increasing r_i but oscillates due to the multivalley nature of Si. Such a theoretical treatment has been proposed by de Sousa and Das Sarma,²⁴ it is therefore interesting to compare our results with theirs.²⁵ Theory predicts the observed angular dependence correctly, but overestimates T_M by about a factor of 3 for both samples. This already-reasonable agreement becomes even better if we take the ratio of T_M between the samples. Indeed, the theoretical ratio of T_M for ^{nat}Si to that for ^{29}Si falls between 11.2 and 11.8, while the experimental ratio lies between 11.2 and 14.4. Given the difficulty in determining the precise T_M due to ESEEM, their calculation is in good agreement with our experiments. Another comparison is to take the ratio of the maximum ($\theta=0^\circ$) and minimum ($\theta\sim 55^\circ$) T_M . Theory yields 2.7 for ^{nat}Si and 2.9 for ^{29}Si , compared with experimental values of 2.0 for ^{nat}Si and 2.1 for ^{29}Si . The larger values in the theory may indicate the presence of an isotropic contribution to T_M , but it is not clear at this stage whether other decoherence mechanisms must be incorporated or an improved theory of nuclear-induced spectral diffusion suffices to explain the discrepancies revealed here. Incorporating non-Markovian nuclear flip-flop processes would certainly be an interesting refinement of the theory, while the stochastic treatment proved valid even for ^{29}Si . It is also noteworthy that recent multiple-pulse NMR studies in Si provide a glimpse into the complicated behavior of this seemingly simple dipolar coupled system.^{26–28} Clearly, more experimental and theoretical investigation is necessary for a full understanding of the phenomena.

We now turn our attention to the remarkable feature of the decay curves: ESEEM. The origin of ESEEM can be described briefly as follows: If the nuclear spin feels, in addition to the external magnetic field, the moderate hf field produced by the electron spin, the nuclear spin precesses around an effective magnetic field which is tilted from the external magnetic field, i.e., m_l is no longer a good quantum number. Due to this state mixing, formally forbidden nuclear-spin-flip transitions ($\Delta m_S = \pm 1, \Delta m_l = \pm 1$) can occur, and interfere with allowed transitions to produce beats in the electron spin echo envelope. In two-pulse experiments for an $S=1/2, I=1/2$ spin system, the modulation contains the ENDOR frequencies ν_+ and ν_- , and their sum and difference $\nu_+ \pm \nu_-$. When many nuclei are coupled to the same electron spin, some combination frequencies are also contained since the two-pulse ESEEM is the product of individual modulation functions.

We analyzed the ESEEM spectra in the frequency domain. Although ESEEM was also observed in ^{nat}Si , we treat only the case of ^{29}Si here because the larger modulation depth in ^{29}Si facilitated the analysis. Also, the modulation depth is strongly angle dependent (Fig. 1), since the degree of state mixing depends on both the position of each nuclear spin and the orientation of the external magnetic field. To obtain a frequency-domain spectrum, the slowly decaying part of a time-domain spectrum was subtracted first, then the remaining modulation was Fourier transformed.²⁹ Figure 3(a) shows the frequency domain spectra at $\theta=0^\circ, 50^\circ$, and

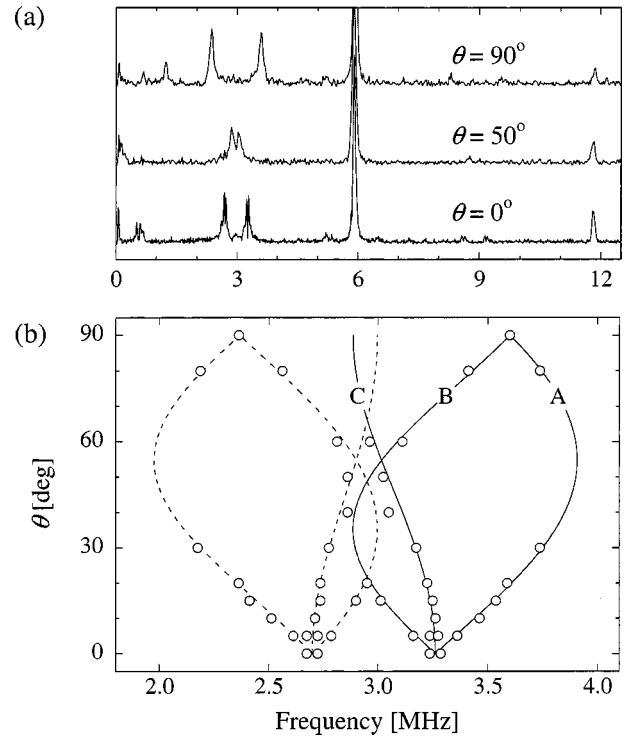


FIG. 3. (a) The frequency domain ESEEM spectra in ^{29}Si at $\theta = 0^\circ, 50^\circ$, and 90° . The vertical axis is shown in an arbitrary unit and shifted for clarity. (b) The orientation dependence of the ENDOR frequencies around 3 MHz. They show a $\langle 111 \rangle$ -axis pattern. The solid (dashed) lines are for ν_+ (ν_-). Which lattice site produces lines A, B, and C is explained in the text.

90° . Peaks around 3 MHz are the ENDOR lines, and their angular dependence is shown in Fig. 3(b), from which we see a $\langle 111 \rangle$ -axis pattern.² The ENDOR frequencies for an axially symmetric hf tensor with an isotropic g factor are given by³⁰

$$\nu_{\pm} = \sqrt{\left(\nu_l \pm \frac{a_{\text{iso}} + b(3 \cos^2 \varphi_i - 1)}{2}\right)^2 + \left(\frac{3b \sin 2\varphi_i}{4}\right)^2},$$

where ν_l is the nuclear Larmor frequency, a_{iso} the isotropic hf coupling constant, b the anisotropic hf coupling constant, and φ_i the angle between \mathbf{B}_0 and the unique axis of the hf tensor. ν_l is calculated to be 2.94 MHz as the gyromagnetic ratio of ^{29}Si nuclei is 8.46 MHz/T. ν_{\pm} calculated with $a_{\text{iso}} = 570$ kHz and $b = 681$ kHz agree well with the experimental results, as shown in Fig. 3(b). In comparison with hf constants obtained from previous cw ENDOR experiments,² the observed peaks are assigned to shell E (111), i.e., four nearest neighbors of the donor. Lines A and B originate from (111) and $(\bar{1}\bar{1}\bar{1})$ sites, respectively. Line C is doubly degenerate, since (111) and $(\bar{1}\bar{1}\bar{1})$ sites locate each other at plane symmetric positions with respect to the $(1\bar{1}0)$ plane. The experimental data corresponding to line C at $\theta=0^\circ$ and 10° split, however. This suggests that the sample was not exactly rotated around the $[1\bar{1}0]$ axis, most likely due to a small misalignment of the crystal. This assumption is supported by

the fact that the ESEEM in ^{nat}Si at $\theta=0^\circ$ did not split (not shown). The strong peak at 5.9 MHz is the sum frequency, but signals from shell A (004) are overlapped. The fourth harmonic is also observed at 11.8 MHz, and the third harmonic is barely visible around 9 MHz. We did not observe the third and fourth harmonics in ^{nat}Si . We also observed tiny peaks around 5.2 MHz throughout the angles tested. They are assigned to shell B (440), but the detailed angular dependence was untraceable. A three-pulse stimulated echo method would be suitable for a more detailed ESEEM study. From the viewpoint of quantum computing, ESEEM clearly leads to quantum-gate errors. For this purpose, time-domain analysis is highly desirable as recently simulated by Saikin and Fedichkin.³¹

In conclusion, we have measured the phase relaxation time T_M of P donor electron spins for ^{nat}Si and ^{29}Si at 8 K. T_M for ^{29}Si is an order of magnitude shorter than that for ^{nat}Si due to much more frequent flip-flops of the host nuclear spins. The orientation dependence of T_M agrees qualitatively with $(M_2)^{-1/2}$ for a 100% ^{29}Si crystal calculated with the method of moment, and quantitatively with the theory of de

Sousa and Das Sarma. Frequency-domain analysis revealed that ESEEM effects originate mainly from the hf interactions between the donor electron and its nearest-neighbor nuclei, as suggested by Saikin and Fedichkin. Our results also provide insights into the localized electrons in III–V materials, such as GaAs, whose lattice sites are full of nuclei with nonzero spin. Their phase relaxation would be severely controlled by nuclear-induced spectral diffusion; therefore, the experimental conditions must be arranged carefully so that the effects of nuclear spins may be suppressed, e.g., high magnetic fields, decoupling pulses, etc. In the near future we plan to prepare a series of samples with different ^{29}Si isotopic composition. Such samples will allow us to carry out systematic relaxation time studies of the electron and nuclear spins as a function of ^{29}Si concentration.

We thank H.-J. Pohl for the ^{29}Si crystal and R. de Sousa for valuable comments and kindly providing his calculation results. This work was supported in part by the Grant-in-Aid for Scientific Research No. 64076215.

*Electronic address: kitoh@appi.keio.ac.jp

¹G. Feher, Phys. Rev. **114**, 1219 (1959).

²E. B. Hale and R. L. Mieher, Phys. Rev. **184**, 739 (1969).

³J. L. Ivey and R. L. Mieher, Phys. Rev. B **11**, 822 (1975).

⁴H. Overhof and U. Gerstmann, Phys. Rev. Lett. **92**, 087602 (2004).

⁵B. E. Kane, Nature (London) **393**, 133 (1998).

⁶R. Vrijen, E. Yablonovitch, K. Wang, H. W. Jiang, A. Balandin, V. Roychowdhury, T. Mor, and D. DiVincenzo, Phys. Rev. A **62**, 012306 (2000).

⁷T. D. Ladd, J. R. Goldman, F. Yamaguchi, Y. Yamamoto, E. Abe, and K. M. Itoh, Phys. Rev. Lett. **89**, 017901 (2002).

⁸J. P. Gordon and K. D. Bowers, Phys. Rev. Lett. **1**, 368 (1958).

⁹A. M. Tyryshkin, S. A. Lyon, A. V. Astashkin, and A. M. Raitsimring, Phys. Rev. B **68**, 193207 (2003).

¹⁰E. Yablonovitch, H. W. Jiang, H. Kosaka, H. D. Robinson, D. S. Rao, and T. Szkopek, Proc. IEEE **91**, 761 (2003).

¹¹T. G. Castner, Jr., Phys. Rev. Lett. **8**, 13 (1962).

¹²T. G. Castner, Phys. Rev. **155**, 816 (1967).

¹³K. M. Itoh, J. Kato, M. Uemura, A. K. Kaliteevskii, O. N. Godisov, G. G. Devyatych, A. D. Bulanov, A. V. Gusev, I. D. Kovalev, and P. G. Sennikov, Jpn. J. Appl. Phys., Part 1 **42**, 6248 (2003).

¹⁴C. P. Slichter, Phys. Rev. **99**, 479 (1955).

¹⁵M. Chiba and A. Hirai, J. Phys. Soc. Jpn. **33**, 730 (1972).

¹⁶K. Sugihara, J. Phys. Soc. Jpn. **18**, 961 (1963).

¹⁷G. Yang and A. Honig, Phys. Rev. **168**, 271 (1968).

¹⁸This tendency has also been suggested by A. M. Tyryshkin and S.

A. Lyon experimentally (unpublished).

¹⁹J. H. Van Vleck, Phys. Rev. **74**, 1168 (1948).

²⁰K. Schaumburg, E. Shabanova, and J. P. F. Sellschop, J. Magn. Reson., Ser. A **112**, 176 (1995).

²¹K. Lefmann, B. Buras, E. J. Pedersen, E. S. Shabanova, P. A. Thorsen, F. Berg Rasmussen, and J. P. F. Sellschop, Phys. Rev. B **50**, 15623 (1994).

²²A. S. Verhulst, D. Maryenko, Y. Yamamoto, and K. M. Itoh, Phys. Rev. B **68**, 054105 (2003).

²³K. M. Salikhov and Y. D. Tsvetkov, in *Time Domain Electron Spin Resonance*, edited by L. Kevan and R. N. Schwartz (Wiley, New York, 1979), Chap. 7.

²⁴R. de Sousa and S. Das Sarma, Phys. Rev. B **68**, 115322 (2003).

²⁵Theoretical values given here were provided by R. de Sousa (private communication).

²⁶S. Watanabe and S. Sasaki, Jpn. J. Appl. Phys., Part 2 **42**, L1350 (2003).

²⁷A. E. Dementyev, D. Li, K. MacLean, and S. E. Barrett, Phys. Rev. B **68**, 153302 (2003).

²⁸T. D. Ladd, D. Maryenko, Y. Yamamoto, E. Abe, and K. M. Itoh, quant-ph/0309164 (unpublished).

²⁹In the present experiments, a step of τ was set to 40 ns; hence, the Nyquist frequency is 12.5 MHz. As the data were taken from $\tau=320$ ns, all the modulation components that decayed within 320 ns cannot be recovered in the frequency-domain spectra.

³⁰A. Schweiger and G. Jeschke, *Principles of Pulse Electron Paramagnetic Resonance* (Oxford University Press, Oxford, 2001).

³¹S. Saikin and L. Fedichkin, Phys. Rev. B **67**, 161302R (2003).